

ANALYSIS OF PREARCING TIME-CURRENT CHARACTERISTIC OF FUSELINKS.

C. Garrido

and

J. Cidras

Dept. of Electrical Engineering, University of Vigo, P.O.Box 62, 36280-VIGO (Spain).

1. SUMMARY.

This paper presents a model for the calculation of the prearcing time in fuse-links, based on the solution of the equations of electrical potential, current density and heat diffusion, by means of the approximation of the partial derivatives through central finite differences. The variations in the values of the different parameters induced by temperature are taken in consideration. Due to the non-linearity of the equations the solution is obtained through an iterative or Gaus-Seidel relaxation process.

2. INTRODUCTION

Gauged conductors (fuse-links) are used in the industry as a means of protecting equipment and installations against the sudden occurrence of current overloads or short-circuits. In order to adequately employ fuse-links as protecting elements one has to know their characteristic intensity/time curve. Normally experimental laboratory test methods are used to obtain such characteristic curves, which bring about a substantial loss of both time and rejected materials. Consequently, a theoretical model which could allow the accurate prediction of the performance of a fuse-link under different conditions of loading and under short-circuit would undoubtedly have a great potential appeal for designers and testers at fuse-link factories.

Due to the fact that the fuse element usually has complicated geometrical forms (see Fig. 1) and that as a rule such parameters as the electric resistivity, thermal conductivity and specific heat vary with temperature, the analytical techniques approach to the study is not possible but it is necessary to appeal to the numerical calculus to be able to build a valid theoretical model of the performance of the fuse.

Several authors have proposed different models for determining the prearcing-time. Leach et al.¹ developed a model which estimates the distribution of the current density by means of the approximation through finite differences of the electric continuity equation. The current density so estimated is used to find out by application of the law of Ohm, the heat generated inside the fuse, which is also expressed by the energetic equation $Q=Cp.m.dT$, where Q is the

heat generated, Cp is the specific heat, m is the mass and dT is the thermal increment produced by the heat generated. Wilkins and others² brought forward a model which uses the approximation of the partial derivatives through finite differences to solve the equations of the electric continuity and heat diffusion. In this model they take into consideration neither the eventual variation of the aforementioned parameters due to temperature nor the eventual heat losses from the fuse element to the surrounding medium (the filling material, usually sand or quartz powder) and to the ceramic core of the fuse.

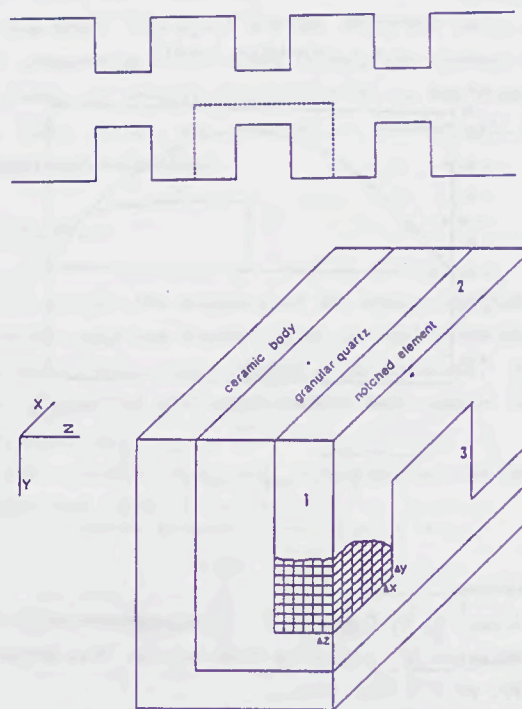


Fig.1: Typical fuselink element, symmetrical part of an element used in our model and finite-difference mesh.

Considering that the electric resistivity of the fuse, the thermal conductivity and the specific heat of the fuse, of the filling material and of the ceramic core vary with temperature, this paper presents a model which uses the method of the finite differences to solve the equations of the electric potential, current density and heat diffusion to estimate the prearcing time in fuses, taking into consideration the variability of the said parameters with variations of temperature.

3. MODEL DESCRIPTION.

Considering that the fuse used for the experimental test of the theoretical model presents the shape shown in Fig. 1, by symmetry the part of the fuse shown on the said figure has been used. Although fuses usually present a cylindrical shape, in order to have a simpler modeling we have approximated the cylindrical surfaces which separate the quartz from the ceramic core and the latter from the environment by flat surfaces which contain them. For the evaluation of the prearcing time it is necessary to solve the equation of heat in the fuse using as a source of energy that produced by the Joule effect of current density. Consequently it is necessary to calculate first of all this density.

3.1 Distribution of currents in the fuse.

Considering that a fuse with uniform thickness is used, the current density J presents components J_x and J_y in directions x & y respectively, which are related to the components of the electric field E by:

$$\begin{aligned} J_x &= E_x/\rho \\ J_y &= E_y/\rho \end{aligned} \quad (1)$$

where ρ is the electric resistivity of the material of fuse and E_x & E_y are the components of the electric field in the direction x & y respectively. Bearing in mind the relation existing between the electric field and the electric potential V : $E = -\text{grad}.V$ and that the divergence of the current density is null (there are neither load sources nor sinks) substituting in (1) gives:

$$\begin{aligned} \text{div}.J &= -\text{div}.\left(\frac{\text{grad}.V}{\rho}\right) = 0 \\ J_x &= -\frac{1}{\rho} \frac{\partial V}{\partial x} \\ J_y &= -\frac{1}{\rho} \frac{\partial V}{\partial y} \end{aligned} \quad (2)$$

The resistivity varies from point to point in the fuse as temperature changes [$\rho = \rho(T(x,y,z,t))$], and bringing this over to equation (2) and operating results:

$$\begin{aligned} \frac{1}{\rho} \nabla^2 V + \nabla\left(\frac{1}{\rho}\right) \cdot \nabla V &= 0 \\ \frac{\partial(1/\rho)}{\partial T} \left[\frac{\partial T}{\partial x} \frac{\partial V}{\partial x} + \frac{\partial T}{\partial y} \frac{\partial V}{\partial y} \right] + \frac{1}{\rho} \left[\frac{\partial^2 V}{\partial x^2} + \frac{\partial^2 V}{\partial y^2} \right] &= 0 \end{aligned} \quad (3)$$

To solve equation (3) the following boundary conditions have been assumed:

- 1) on the frontal surfaces which connect the fuse

element with the remaining elements (marked "1" on Figure 1) the distribution of current density is not affected by the presence of the restriction (lengthwise dimensions are usually big enough to hold this as a fact) whereby the current density is constant on each elementary surface, each component presenting the values given by:

$$\begin{aligned} J_x &= -\frac{1}{\rho} \frac{\partial V}{\partial x} = \pm \frac{I}{2 \cdot N \cdot \Delta S} \\ J_y &= \frac{\partial V}{\partial y} = 0 \end{aligned} \quad (4)$$

where N is the number of elementary areas into which the surface is divided, ΔS is its area and I is the intensity that flows through the fuse. The + sign in the J_x equation corresponds to the current in-flow surface and the - sign to the current out-flow surface. The division by 2 on the J_x expression is due to the fact that only one half of the current in and out-flow surfaces is considered.

2) On those boundary surfaces which are parallel to the x axis (marked "2" on Figure 1) the y component of the current density is null:

$$J_y = 0 \Rightarrow \frac{\partial V}{\partial y} = 0 \quad (5)$$

3) Finally, on those boundary surfaces which are parallel to the y axis (marked "3" on Figure 1) the x component of the current density is null:

$$J_x = 0 \Rightarrow \frac{\partial V}{\partial x} = 0 \quad (6)$$

Through a discretization on the fuse as shown on Fig.1, the approximation of the partial derivatives through central finite differences² the electrical potential on a point of discrete coordinates (i,j) can be obtained and from here the components of the current density are calculated by means of equation 2

3.2 Temperature distribution in the fuse.

To accurately ascertain the distribution of temperatures in the fuse it is necessary to solve the heat diffusion equation, as follows:

$$\begin{aligned} d \cdot C_p \frac{\partial T}{\partial t} &= \nabla(K \nabla T) + Q_v = \\ K \left[\frac{\partial^2 T}{\partial x^2} + \frac{\partial^2 T}{\partial x^2} + \frac{\partial^2 T}{\partial x^2} \right] + \frac{\partial K}{\partial T} \left[\left[\frac{\partial T}{\partial x} \right]^2 + \left[\frac{\partial T}{\partial x} \right]^2 + \left[\frac{\partial T}{\partial x} \right]^2 \right] + Q & \end{aligned} \quad (7)$$

where d is the density of the material, C_p and K are its specific heat and thermal conductivity and Q_v represents the energy generated per unit of volume

and per unit of time in the material. Both C_p and K may vary from point to point as temperature changes. To solve equation (7) the following boundary conditions have been assumed as true:

1) By symmetry there is no loss of heat (equal heat flows in both directions) on the surfaces which separate the part under examination from the rest of the fuse, for which reason:

$$\frac{\partial T}{\partial l} = 0 \quad (8)$$

where l is normal to the separating surfaces. The eventual losses through the external surface of the ceramic core of the fuse are not considered, whereby equation (8) is used for this surface.

This hypothesis is acceptable enough considering that the fuse element is surrounded by quartz grains, which present a very low thermal conductivity thus limiting the heat which passes over to the ceramic core.

2) In the separating surfaces between different materials (copper, quartz and ceramic) the equality of heat-flows in both directions is satisfied:

$$K_1 \frac{\partial T}{\partial l} = K_2 \frac{\partial T}{\partial l} \quad (9)$$

where K_1 and K_2 are the thermal conductivities of the medium 1 and 2 respectively and l is the normal to the separating surface.

The internal heat generation is due in this case to the Joule effect of the electrical flow and is represented by:

$$Q_v = \rho (J_x(i,j)^2 + J_y(i,j)^2) \quad (10)$$

Bearing in mind the variation in thermal conductivity induced by temperature changes, the new temperature $T(i,j,k)$ on points of discrete coordinates (i,j,k) after a discrete interval of time Δt , can be ascertained through the discretization of (7) around central points.

The distribution of the potential with the temperature existing at the beginning of each discrete interval of time or iteration is ascertained through the discretization of equation (3). From the discretization of (2) the current densities can be ascertained and they are used in equation (10) to calculate Q_v , which applied in (7) permits the obtainment of the new temperature on each point at the end of the interval. The new temperatures substitute those had at the beginning and the process is repeated in subsequent iterations. The process ends

when the fusion temperature of the copper fuse element is reached, thus determining the prearcing time.

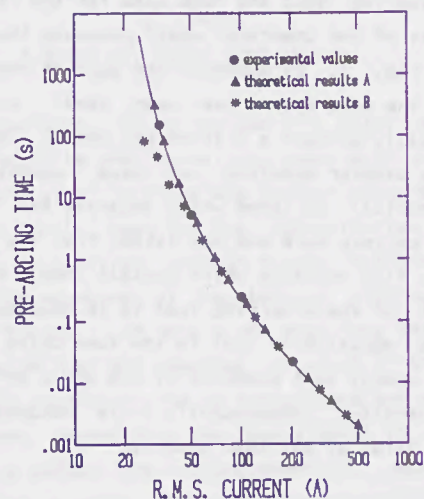


Fig.2: Prearcing time-current curve for a 15 A protection fuselink, 50 Hz symmetrical sinusoidal current.

Table 1: Parameter values of copper used in the model. K =thermal conductivity; ρ =resistivity; C_p =specific heat; d =density.

$\rho(\Omega m) = 1.785 \times 10^{-8} [1 - 4.1 \times 10^{-5}(T-20) + 0.43 \times 10^{-6}(T-20)^2]$	[4]
$K (W/m^2K) = 418.38 - 6.16 \times 10^{-5} T$	[5]
$K (W/m^2K) = 400$	[5]
$C_p (J/Kg^{\circ}K) = 358 + 0.962 T$	[6]
$d (Kg/m^3) = 8960$	[7]

4. RESULTS.

Figure 2 shows the experimental values and the theoretical results obtained for a fuse with 15 A nominal intensity. Values of parameters are shown on Table I. The theoretical results have been calculated via two different models: through model developed under paragraph 3 Case A results have been reached, whereas on Case B the thermal losses transferred to the quartz powder and the ceramic core have not been taken into account. As shown, both models render identical results for intermediate and high intensities (typical short-circuit values), which coincide with those obtained in laboratory experiments, whereas for intensities close to the nominal intensity of the fuse (typical overload values) the results obtained with the complete model are similar to the experimental values, while those obtained in case B present differences which grow as the intensity values decrease. This results show that the thermal losses by transfer to the surrounding materials of the fuse element are irrelevant for short-

circuit intensities due to the short prearcing times, while they grow bigger as the overload intensity approaches the fuse nominal value due to the longer prearcing times. It is consequently evident that such losses have to be taken into consideration if an accurate model of the performance of a fuse is to be built.

It is interesting to note what effects have some parameters on the performance of the model. Figure 3 shows the temperature reached in the middle of the restriction zone as a function of the current flow-time considering one value for the thermal conductivity of copper as constant and the other as variable. The intensity is 50 A while the remaining parameters vary with temperature. As shown, for short times (low temperatures) similar results are obtained with both conductivity values, and the gap grows with time (and so does the temperature as a result thereof) to the extent that the estimation of the prearcing time with one or the other value of conductivity differ in more than 20%, the minimum value being in no case under 8%. This indicates that if the model is to be adequate the variability of the thermal conductivity of copper as the temperature changes has to be taken into account. Of much less importance is the existence or not of variability in the thermal conductivity of the quartz or the ceramic core because the temperatures on these materials are much lower than those on copper, which implies that the variations in conductivity are so small that they have very little effect on the estimation of the prearcing time.

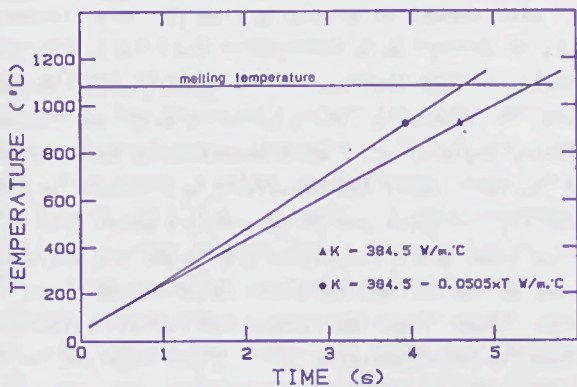


Fig.3: Temperature at the center of the restriction zone as a function of the time for two different values of the copper thermal conductivity.

Figure 4 shows the effect of the circuit closing angle on the thermal development in the middle of the restriction. The intensity is 300 A, using circuit closing angles of 0, 40 and 82° for a sinus function.

A symmetric short-circuit has been assumed, which means that the circuit created presents no reactance.

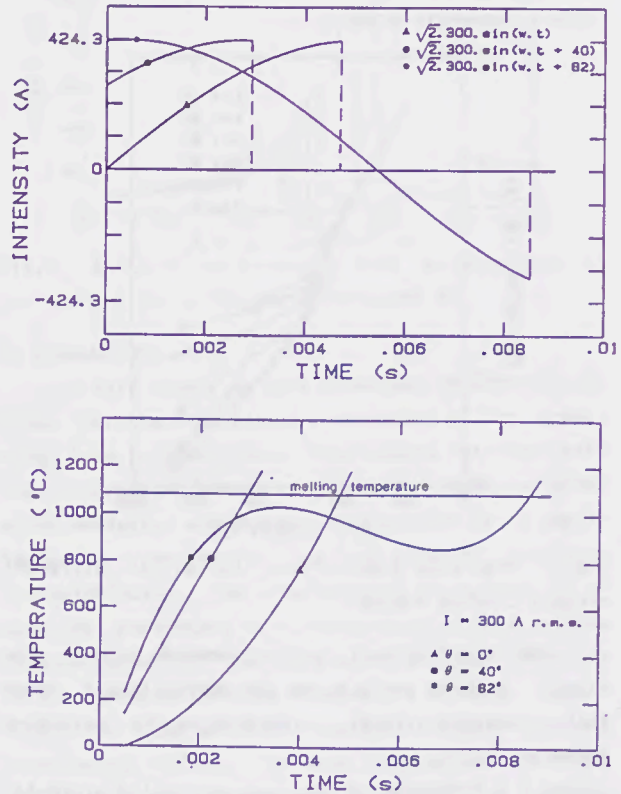


Fig.4: Current intensity and temperature at the center of the restriction zone as a function of the time for three different values of the circuit closing angle.

As shown, depending on the moment the short-circuit is produced (circuit closing angle) the prearcing time obtained varies substantially with differences which are larger than 200% for values obtained with circuit closing angles of 40 and 82°. While for circuit closing angles of 0 and 40° the fusion takes place in the first half-period of the intensity wave, for the circuit closing angle of 82° the fusion cannot take place during the first half-period owing to the high initial stage value, wherefore the temperature -after decreasing slightly- reaches the fusion value (1083 °C) during the 2nd half-period of the intensity wave. This decrease in the temperature is due to the fact that when the intensity wave reaches the null and close to null values, the thermal losses are bigger than the amount of energy brought by the Joule effect. This is shown in detail in Figure 5, which displays the prearcing times as a function of the r.m.s. current for different values of circuit closing angle. As shown, the prearcing time starts to be affected by the circuit closing angle at intensities close to 150 A and the differen-

ces grow with the short-circuit intensity. This shows that the uncertainty in the time it takes a fuse to open increases considerably as the short-circuit intensity grows.

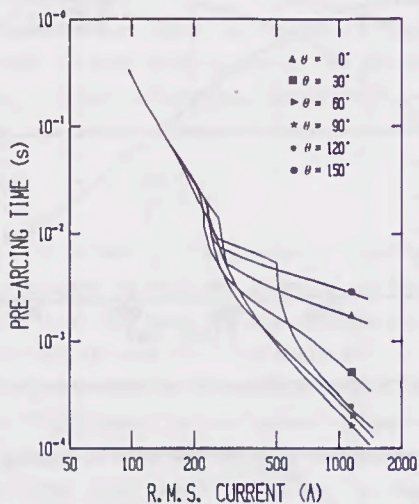


Fig. 5: Pre-arcing time-current curves for different circuit closing angles.

The short-circuit current depends both on the circuit closing angle θ and the short-circuit power factor angle β circuit, according to the following formula:

$$i(t) = 2.I_c[\sin(\omega t + \theta - \beta) - \exp(-\omega t / \tan \beta)] \sin(\theta - \beta) + 2.I \cdot \exp(-\omega t / \tan \beta) \cdot \sin \theta$$

where I_c is the short-circuit permanent current and I is the current which flows through the fuse before the short-circuit. One of the advantages of the fuse as against other protecting elements is the capability of the fuse to limit the maximum value of the transient short-circuit current to a value below its maximum peak value. Figure 6 illustrates this limiting effect (cut-off characteristics) for angles of the short-circuit power-factor of 0, 20 & 78°, which represent the maximum transient peak value as a function of the short-circuit permanent current.

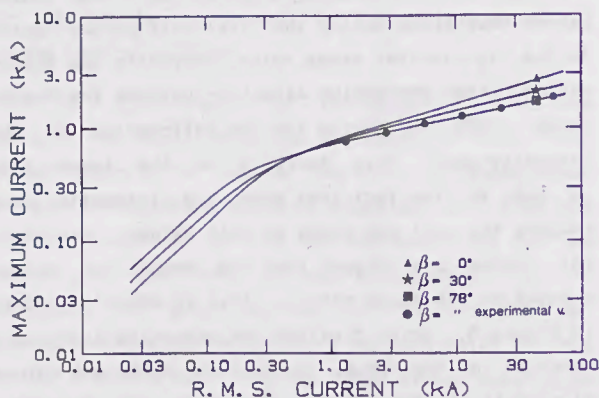


Fig. 6: Fuselink cut-off characteristic for three different short-circuit power-factor angles.

For short-circuit permanent currents under 175, 290 and 350 A, corresponding to angles of 78, 30 and 0° respectively, the fuse exercises no limiting action on the maximum peak transient current due to the fact that the fusion takes place after having reached such a value. Once the limiting effect has started, the maximum value of the thus limited current grows slowly with the increase of the short-circuit permanent current. The limiting effect grows as the impedance short-circuit angle increases. As illustrated the experimental values obtained for an angle of 78° coincide fully with those calculated theoretically.

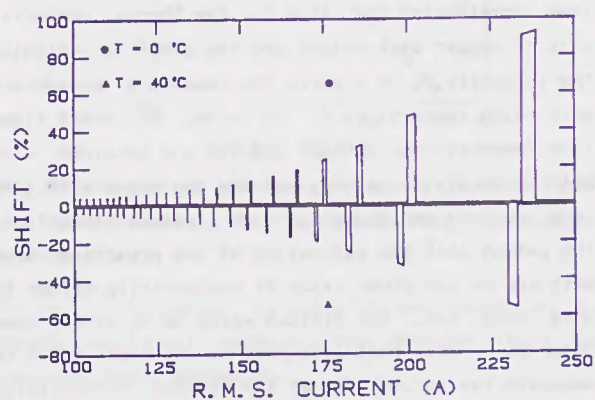


Fig. 7: Shift of the pre-arcing time (with regard to the pre-arcing time for the room temperature of 20°C) as a function of the current for two different room temperatures.

The effect of the room temperature on the modification of the pre-arcing time is illustrated in Figure 7, where the deviation is shown in percentages of pre-arcing time for room temperatures of 0 and 40 °C with respect to pre-arcing time for room temperature of 20 °C, as a function of the r.m.s. current flowing through the fuse. The results shown correspond to symmetric short-circuits with an circuit closing angle of 0°. With exception of some values of current where the deviations are large, in the majority of cases the deviations are about 1%. In those cases where deviations are large, the deviation grows as the current increases up to values close to 100%. Such huge deviations for certain values of intensity (both positive for 0 °C and negative for 40 °C) are due to the fact that while the fuse reaches fusion for a given number of half-periods of the current wave at 20 °C, at 40 °C room temperature it takes a half-period less, whereas it takes one half-period more for room-temperature of 0 °C. As a consequence thereof the deviation increases as the intensity grows since the relative deviation is larger when the number of half-periods taken to reach fusion decreases. On reaching values of intensities

which make the fuse open in times close to or under one fourth of period, these deviations go down about to 1% because then the difference in room temperature is not enough to cause the aperture in the following half-period. This happens with the deviation by 0°C for obviously at the room temperature of 40° it takes only one half-period. For an intensity of 233 A this is illustrated in Figure 8, where the temperature in the middle of the restriction is represented as a function of time for room temperatures of 20 & 40 °C. As shown, while fusion is reached in the first half-period of the intensity wave ($t=0.00775$ s) for the room temperature of 40 °C, for the room temperature of 20 °C fusion takes place in the second half-period of the wave ($t=0.0145$ s). Owing to the difference of 20 ° in room temperature the fusion temperature cannot be reached in the first half-period, although the temperature reached ($T=1067$ °C) is very close to it.

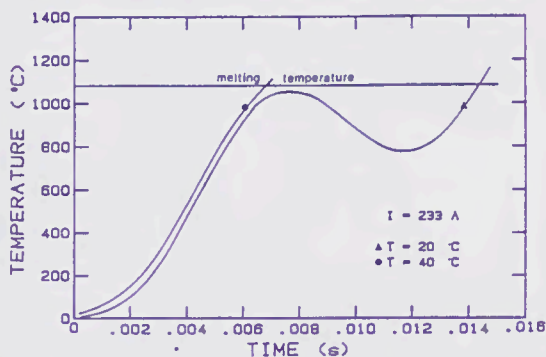


Fig.8: Temperature at the center of the restriction as a function of the time for two different room temperatures.

The effect of variations in thickness of the fuse-element on the prearcing time is shown in Figure 9, where the deviation in prearcing time obtained with a fuse-thickness increased by 5% and the prearcing time with a normal thickness is shown as a function of the r.m.s. current. A room temperature of 20 °C has been assumed. While for intensities over 245 A the deviation in prearcing time is about 7% (because beyond these intensities fusion takes place on both thicknesses within the first wave half-period) at lower intensities the deviation decreases in a discontinuous way after having reached a maximum at 245 A. Such discontinuous decrease is due to the fact that at certain values of intensity fusion is reached within the same half-period on both thicknesses, at other values of intensity fusion takes place one half-period later in the case of the thicker fuse and at other intensities fusion takes place one full period later on the thicker fuse.

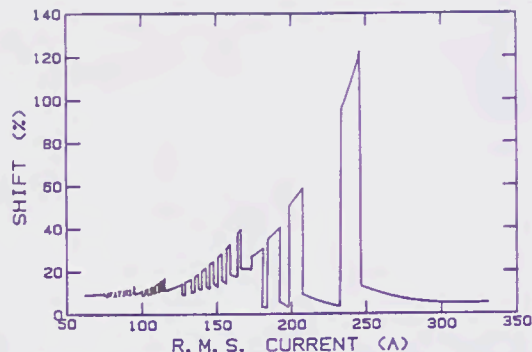


Fig.9: Shift of the prearcing time as a function of the current for a thickness increased 5%.

5. CONCLUSIONS

In this paper, we have presented a mathematical model for the theoretical calculation of the prearcing time in fuse-links. The results obtained with the theoretical model coincide with those obtained experimentally, whereby the model proves to be applicable for the design, test and study of fuse-link characteristics. The consideration of variability of equation parameters with temperature as well as the consideration of thermal losses to the materials which surround the fuse element are of major importance for a perfect coincidence of theoretical and experimental values. The model also allows the study of the influence which the variation of the geometry of the fuse element has in the prearcing time as well as the selection of the material most convenient for the fuse specifications required.

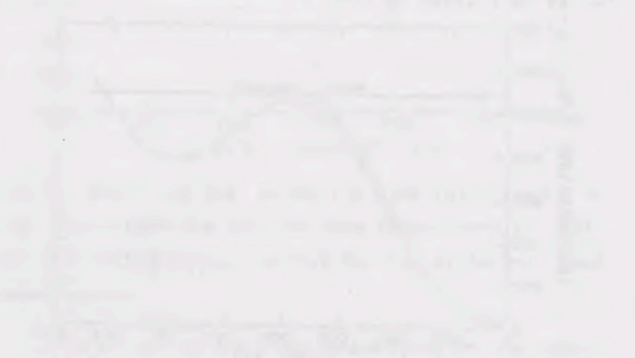
6. REFERENCES

- [1] J.G. Leach, P.G. Newbery y A. Wright, "Analysis of high-rupturing-capacity fuselink prearcing phenomena by a finite-difference method", *Proceeding IEE*, 1973, **120** (9), pp. 987-993.
- [2] R. wilkins and P.M. McEwan, "A.C. short-circuit performance of notched fuse elements", *Proceeding IEE*, 1975, **122** (3), pp.289-292.
- [3] D. Euvrard, "Résolution numérique des équations aux dérivées partielles" Ed. Masson, Paris (1988).
- [4] R.G. Lukac, D.A. Silver, R.A. Hartlein and W.Z. Black, "Optimization of metallic shields for extruded dielectric cables under fault conditions", *IEEE Transactions on Power Apparatus and Systems*, 1984, **PAS-103**, pp.3410-3418.
- [5] R.C. Weast, "Handbook of Chemistry and Physics", Ed. CRC Press, Cleveland, Ohio (1974).
- [6] D.E. Gray, "American Institute of Physics Handbook", Ed. McGraw-Hill, New York (1972).
- [7] R.E. Bolz and G.L. Tuve, "Handbook of tables for Applied Engineering Science", Ed. CRC Press, USA (1972).



The graph displays a series of peaks, with the most prominent one occurring at approximately 40% of the time axis. The amplitude of this peak is significantly higher than the others. The subsequent peaks are smaller and occur at regular intervals, suggesting a periodic or sequential process. The baseline of the graph shows some minor fluctuations, but remains relatively stable throughout the duration shown.

The data points from the graph indicate a clear trend of increasing amplitude followed by a decrease and then a series of smaller, regular peaks. This pattern could represent a damped oscillation or a series of discrete events. The time intervals between the peaks are consistent, which supports the idea of a periodic phenomenon. The overall behavior is characteristic of a system that has been excited and is now decaying or settling into a steady state.



This graph shows a similar pattern to the one on the left, but with a lower overall amplitude and longer time intervals between peaks. The most significant peak is also centered around the 40% mark on the time axis. The regular spacing of the smaller peaks suggests a consistent periodicity. The lower amplitude might indicate a different level of excitation or a different system parameter compared to the first graph.

Session 6A
FUSE TESTING

THE HISTORY OF THE
CITY OF BOSTON

